NMR spectroscopy is a valuable tool in elucidating the internal structure and the electronic properties of semiconductor and metal clusters.[15r,16] In the case of HgTe clusters, no detectable NMR resonances or spin echoes in either ^{199}Hg and ^{125}Te NMR could be found, in contrast to the spectra of polycrystalline mercury telluride powder prepared from bulk material, which gives the expected single-line resonances in both ^{199}Hg and ^{125}Te. Experiments on CdSe clusters clearly showed resonances due to core and surface ^{77}Se atoms.[16] We attribute the lack of signal in HgTe clusters to line broadening which occurs in small particles (as was seen in the ^{77}Se NMR spectra of cadmium selenide clusters). Possible reasons for such broadening are as follows: (1) a wide chemical shift distribution due to the different chemical environments of surface and core atoms. Measurements of the precursor $Hg(TePh)_2$ ("monomeric" HgTe) in solution and in the solid state illustrate this effect: a 20% solution of $Hg(TePh)_2$ in triethylphosphine shows a narrow ^{199}Hg line (line width 120 Hz at -640 ppm relative to neat dimethylmercury). In solid-state NMR of amorphous $Hg(TePh)_2$ powder this resonances broadens to 56 000 Hz. (2) Knight shift distribution.[17] (3) Boundary-induced charge oscillations, such as those reported for lead particles smaller than 340 Å.[18]

(16) Thayer, A. M.; Steigerwald, M. L.; Duncan, T. M.; Douglas, D. C. *Phys. Rev. Lett.* **1988**, *60*, 2673.
(17) Townes, C. H.; Herring, C.; Knight, W. D. *Phys. Rev.* **1950**, *77*, 852.
(18) Hines, W. A.; Knight, W. D. *Phys. Rev. B* **1971**, *4*, 893.

Conclusions

We have used bidentate phosphines to isolate crystalline derivatives of the group II-VI precursor molecules $M(EPh)_2$-DEPE. These complexes can be thermally decomposed to give solid group II-VI compounds without degradation of the organic ligands. In select cases, nanometer-sized group II-VI clusters can be isolated at intermediates in the thermolysis reaction. Decomposition reactions can also be driven photolytically: $Hg(TeBu)_2$ is thermally stable at room temperature but decomposes upon exposure to room light to give first nanoclusters of HgTe and then bulk HgTe.

Acknowledgment. We are grateful to F. Padden for his assistance in learning the use of the electron microscope and to him and A. Lovinger for the use of this equipment.

Registry No. $Zn(SPh)_2$, 6865-39-0; $Zn(SePh)_2$, 120138-28-5; $Cd(SPh)_2$, 21094-83-7; $Cd(SePh)_2$, 120138-29-6; $Cd(TePh)_2$, 123676-75-5; $Hg(TePh)_2$, 97671-41-5; $[Zn(SPh)_2DEPE]_2$, 127915-92-8; $[Zn(SePh)_2DEPE]_2$, 127915-93-9; $[Cd(SPh)_2DEPE]_2$, 127915-94-0; $[Cd(SePh)_2DEPE]_2$, 127915-95-1; $[Cd(TePh)_2DEPE]_2$, 127915-96-2; $[Hg(TePh)_2DEPE]_2$, 127915-97-3; $[Cd(SePh)_2]_2DMPE$, 127915-98-4; $[Hg(TePh)_2]_2DMPE$, 127915-99-5; $[Cd(SePh)_2]_2DEPE$, 121073-86-7; ZnS, 1314-98-3; ZnSe, 1315-09-9; CdS, 1306-23-6; CdS, 1306-24-7; CdTe, 1306-25-8; HgTe, 12068-90-5.

Supplementary Material Available: Tables listing thermal parameters, significant distances and angles, and powder diffraction patterns of the molecular precursors (8 pages); table of calculated and observed structure factors (14 pages). Ordering information is given on any current masthead page.

Europium Intercalation Chemistry: Novel Behavior in TiS_2 Prepared at 500 °C

V. Cajipe, P. Molinié, A. M. Marie, and P. Colombet*

Institut de Physique et Chimie des Matériaux, CNRS-UMR 110, 2 rue de la Houssinière, 44072 Nantes Cedex 03, France

Received February 12, 1990

Eu intercalation compounds of TiS_2 prepared from the elements at 500 °C were synthesized via the liquid ammonia technique and studied by using X-ray diffraction, magnetic susceptibility measurements, and EPR. Intercalation is found to occur much more rapidly than in the case of TiS_2 prepared at higher temperatures (>600 °C); the products are also magnetically different. Data on the pristine disulfide imply that TiS_2 (500 °C) has less defects and is more stoichiometric than TiS_2 (>600 °C). This subtle distinction is proposed to account for the dramatically faster intercalation reaction and the dissimilar behavior of the resulting compounds.

Introduction

Since TiS_2 was first prepared by Berthier[1] in 1832, its existence as a stoichiometric semiconductor[2,3] and the origin of its observed metallic behavior[4-7] have been intensely disputed. Research on its numerous intercalation compounds[8] and its application as cathodes in secondary batteries[9] has likewise been vigorous. The availability of maximally stoichiometric TiS_2 has been crucial for scientific, synthetic, and technological purposes so that various procedures for its preparation have been developed.[3,10-12]

Both TiS_2 and $TiSe_2$ exhibit the CdI_2 (1T) layered structure[13] wherein the anions are hexagonally close packed and the Ti occupies half of the octahedral sites, thus

(1) Berthier, M. P. *Ann. Chim. Phys.* **1832**, *50*, 372.
(2) Benard, J.; Jeannin, Y. *Adv. Chem. Ser.* **1963**, *39*, 191.
(3) Thompson, A. H.; Gamble, F. R.; Symon, C. R. *Mater. Res. Bull.* **1975**, *10*, 915.
(4) McTaggart, F. K.; Wadsley, A. D. *Aust. J. Chem.* **1958**, *11*, 445.
(5) Conroy, L. E.; Park, K. C. *Inorg. Chem.* **1968**, *7*, 459.
(6) Friend, R. H.; Jérome, D.; Liang, W. Y.; Mikkelsen, J. C.; Yoffe, A. D. *J. Phys. C: Solid State Phys.* **1977**, *10*, L705.
(7) Chang, A. T.; Molinié, P.; Sienko, M. J. *J. Phys. (Paris)* **1978**, *C6*, 1070.
(8) Friend, R. H.; Yoffe, A. D. *Adv. Phys.* **1987**, *36*, 1.
(9) Whittingham, M. S. *J. Solid State Chem.* **1979**, *29*, 303.
(10) Danot, M. Thesis, Nantes, France, 1973.
(11) Thompson, A. H.; Gamble, F. R. *U.S. Patent* **1976**, 3,980,761.
(12) (a) Whittingham, M. S.; Panella, J. A. *Mater. Res. Bull.* **1981**, *16*, 37. (b) Winn, D. A.; Steele, B. C. H. *Mater. Res. Bull.* **1976**, *11*, 551.
(13) Hulliger, F. *Structural Chemistry of Layer-Type Phases*; Levy, F., Ed.; Reidel: Dordrecht, 1976; p 219.

0897-4756/90/2802-0409$02.50/0

yielding alternating filled and empty planes. These empty planes are the so-called van der Waals (vdW) gaps into which guest atoms or molecules may intercalate. The electronic structures of these two dichalcogenides are intimately related. The indirect optical gap expected to occur between the valence bonding states and the nonbonding d-like conduction orbitals becomes very small in these compounds so that they have been viewed either as small-gap semiconductors or semimetals with a small band overlap.[14]

It is now widely accepted[15] that TiS_2 is an extrinsic semiconductor, particularly since Friend et al.[6] showed the Hall coefficient to be pressure independent (in contrast to the semimetal $TiSe_2$ case). Various models have been used to calculate the band structure,[14,16] and a gap of 0.2–1 eV has been found. Angle-resolved photoemission experiments[14] give a value of 0.2 eV, which matches the discrete variational LCAO results;[17] this is smaller than the usual band calculation uncertainty and explains the ambiguity of previous results.

The nature of the extrinsic carriers responsible for the metallic behavior has also been difficult to determine. The simplest assumption is that real TiS_2 contains defects in the form of Ti atoms that appear in the vdW gap due to (i) a slight, energetically inevitable metal excess or (ii) the formation of intralayer Ti vacancies[18] even in nominally stoichiometric TiS_2. Experiments on the best (i.e., most stoichiometric) single crystals yield a carrier concentration[19] of $\approx 1.4 \times 10^{20}$ cm^{-3}, which implies a 0.2% Ti *excess* assuming each extra Ti to be tetravalent. The corresponding stoichiometry would then be $Ti_{1.002}S_2$, in fair agreement with a recent chemical analysis study[20] which concluded that TiS_2 is always slightly metal-rich and that the conductivity is entirely attributable to excess Ti. The metallic character of TiS_2 has likewise been confirmed by magnetic susceptibility studies[3,21] which give a constant Pauli paramagnetism $\chi = (9 \pm 2) \times 10^{-6}$ emu mol^{-1}.

It should be noted that all the physical measurements cited above were performed on TiS_2 prepared at 600–640 °C from Ti wire and elemental sulfur in slightly nonstoichiometric proportions, i.e., following the complex procedure developed by Thompson and others[3,11,20] (=TiS_2 (>600 °C)). At such temperatures single crystals large enough for transport experiments can be grown. TiS_2 can, however, be synthesized in one step at lower (500–550 °C) temperatures by reacting essentially stoichiometric amounts of titanium sponge or powder and sulfur[10,12a] (=TiS_2 (500 °C)). The resulting compound is finely divided and has no metallic luster. It has been pointed out that since the intercalation reaction occurs at the crystallites' edges, the small aspect ratio (basal plane dimension to thickness) of TiS_2 (500 °C) implies an optimization of the intercalation rate.[12a]

The present work is a detailed study of Eu intercalation in TiS_2 (500 °C). Our results are in disagreement with those of previous studies which used TiS_2 (>600 °C) as the host material,[22] specifically in that we find the intercalation to proceed much more rapidly and the intercalated species to be less oxidized (more Eu^{2+} than Eu^{3+}) and magnetically different. An explanation of these discrepancies is attempted vis-à-vis a comparison of the properties of the starting disulfide. Also presented is a description of new structural features found in variant preparations of Eu-intercalated TiS_2.

Experimental Methods

Sample Preparation. TiS_2 was synthesized by the direct reaction of stoichiometric amounts of the elements (S, 99.99%, Koch Light, and Ti in powder form 99.99%, Pierce). The titanium–sulfur mixture, sealed in an evacuated (10^{-5} Torr) glass tube, was gradually heated to T = 500 °C, held at this temperature for 2 weeks, and then air-quenched.

As in previous studies,[22] $Eu_{0.10}(NH_4)_{y'}(NH_3)_{y''}$ TiS_2 intercalation compounds were prepared by condensing $\approx$10 cm^3 of sodium-dried ammonia (99.99%, from Air Liquide) over the disulfide and 20–30 mg of Eu metal (high purity, Ames Laboratory, Iowa State University) in the same leg of a Pyrex h-tube. The TiS_2 used was either already ammoniated (yielding ammonia preintercalated Eu compounds) or in pristine form (for cointercalated Eu and ammonia). The h-tube is then sealed, and the leg containing the reactants is immersed in a 228 K alcohol bath and agitated every 15 min. Contact between ammonia and Eu metal above the bath temperature was avoided to prevent the formation of the amide $Eu(NH_2)_2$; all glassware was carefully cleaned with a hydrofluoric acid based solution and distilled water for the same reason.[23] The europium–disulfide intercalation reaction is considered complete when the blue color characteristic of solvated electrons disappears. The residual liquid NH_3 is then decanted/condensed into the second leg, and the intercalate is sealed off and annealed at room temperature for 2 to several days before characterization. No visible (ochre color on TiS_2 particles) or X-ray diffraction evidence for the presence of $Eu(NH_2)_2$ was found in the compounds described in this paper.

$Eu_{0.10}TiS_2$ was obtained by thermal deintercalation of ammonia from the $Eu_{0.10}(NH_4)_{y'}(NH_3)_{y''}$ TiS_2 precursors at 350–430 °C under vacuum. The compounds' NH_3 content was simultaneously determined by pressure measurements that reveal the ammonia deintercalation to be either a single (y' = 0) or two-step process (one step at 70–120 °C followed by another at 300–350 °C). The second step[21] is associated with the departure of NH_3 and H_2 produced upon removal of NH_4^+.

Air-sensitive materials were at all stages handled in an argon-filled glovebox (<10 ppm H_2O and O_2).

Measurement Techniques. X-ray powder patterns from Ar-sealed Lindemann capillary samples were recorded at room temperature with an INEL diffractometer (Cu $K\alpha_1$) equipped with a curved 120° linear detector and calibrated with a Si standard. Electron microscopy on pristine TiS_2 was performed with either a JEOL or Philips apparatus working at 100 and 300 kV, respectively. The magnetic susceptibility (χ) was measured at 8 or 18 kG using $TbPd_3$-calibrated Faraday devices. The compounds were also examined at T = 100–300 K with a Brüker ER200D electron paramagnetic resonance (EPR) spectrometer operating at X-band. Intercalated samples were sealed under vacuum in quartz containers suitable for both susceptibility and EPR measurements.

Results and Discussion

Pristine TiS_2. The TiS_2 we prepared at 500 °C is a fine powder with a dark green color. Sieving and a visual assay give particle sizes between <50 and 900 μm, with the majority falling in the 50–300-μm range, while electron micrographs reveal the presence of well-formed <1-μm hexagonal platelets. This range of sizes is comparable to that found in TiS_2 prepared in two steps and at higher temperatures[11] and not significantly different from that

(14) Doni, E.; Girlanda, R. In *Electronic Structure and Electronic Transitions in Layered Materials*; Grasso, V., Ed.; Reidel: Dordrecht, 1986; p 3.
(15) Kukkonen, C. A.; Kaiser, W. J.; Logothesis, E. M.; Blumenstock, B. J.; Shroeder, P. A.; Faile, S. P.; Colella, R.; Gambold, J. *Phys. Rev.* **1982**, *B24*, 1691.
(16) Wilson, Y. A.; Yoffe, A. D. *Adv. Phys.* **1969**, *18*, 193.
(17) Zunger, A.; Freeman, A. J. *Phys. Rev.* **1977**, *B16*, 906.
(18) Wilson, J. A. *Phys. Status Solidi* B **1978**, *86*, 11.
(19) Klipstein, P. C.; Friend, R. H. *J. Phys. C* **1984**, *17*, 2713.
(20) McKelvy, M. J.; Glaunsinger, W. S. *J. Solid State Chem.* **1987**, *66*, 181.
(21) Bernard, L.; McKelvy, M.; Glausinger, W. S.; Colombet, P. *Solid State Ionics* **1985**, *15*, 301.
(22) (a) Hsu, S. P.; Glausinger, W. S. *J. Solid State Chem.* **1987**, *67*, 109. (b) Hsu, S. P.; Glaunsinger, W. S. *Mater. Res. Bull.* **1986**, *21*, 1063.

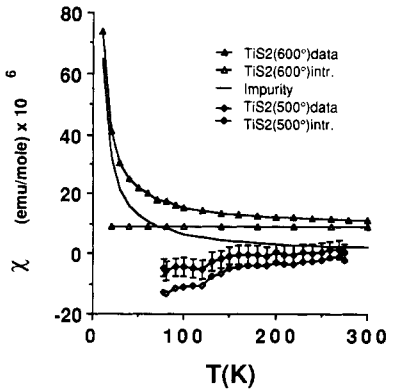

Figure 1. TiS_2 magnetic susceptibility measured at ca. 20 kG. The intrinsic (intr) susceptibility is obtained after correcting the data for paramagnetic impurities.

of the disulfide used in earlier intercalation studies.[20,23] Complete oxidation to TiO_2 gives a composition corresponding to $Ti_{1.001(4)}S_2$, which is essentially equivalent to that of the most stoichiometric higher temperature preparations.

Electron diffraction demonstrates the ubiquity of single crystals in repeated samplings of the powder. A least-squares refinement of the X-ray powder pattern yields a = 3.4058 (7) Å and c = 5.693 (1) Å. These values are slightly smaller than but consistent with those found for TiS_2 (>600 °C) in previous studies.[3] For a more direct comparison of the lattice parameters, X-ray powder diffraction measurements were made under identical conditions on a TiS_2 (>600 °C) sample. These data refine to basically the same a (=3.4054 (7) Å) and a slightly larger c (=5.697 (2) Å).

The dull appearance of TiS_2 (500 °C) contrasts markedly with the golden color of TiS_2 (>600 °C). Since the Ti powder used in the present work has a larger surface area than the Ti wire of the >600 °C preparations,[20,22] it would seem that the difference in color may be due to the higher impurity levels expected to be found in the former. "Gold" TiS_2 can however also be synthesized from the same Ti powder upon following the TiS_2 (>600 °C) recipe, and dark green TiS_2 from Ti wire in a single step at 500–550 °C.

The lusterlessness of TiS_2 (500 °C) is, as a matter of fact, consistent with its other nonmetallike features. Figure 1 illustrates the magnetic susceptibility of TiS_2 (500 °C) (this work) and TiS_2 (>600 °C).[21] χ for TiS_2 (>600 °C) is found to be temperature-independent and equal to $(9 \pm 2) \times 10^{-6}$ emu mol^{-1} after the contribution from paramagnetic impurities ($J = {}^5/_2$, 148 ppm) is subtracted. Since the impurity signal comes mainly from iron in titanium and the purity of the Ti powder used in this work at best equals that of the Ti wire used for TiS_2 (>600 °C), applying the same correction would be an underestimation. The intrinsic susceptibility thus found for TiS_2 (500 °C) is smaller than that for TiS_2 (>600 °C) and exhibits a tendency to decrease at lower T: $\chi = (-2 \pm 3) \times 10^{-6}$ emu mol^{-1} at room temperature and equals $(-13 \pm 3) \times 10^{-6}$ emu at 77 K. Moreover, TiS_2 (500 °C) gives an evidently less metallic response to microwave radiation in the EPR spectrometer cavity than does TiS_2 (>600 °C).

Intercalation Reaction. Eu intercalation at 228 K is rapidly achieved in TiS_2 (500 °C): it is completed within 1 h for the cointercalated case and at most 3 h for the preintercalated. This reaction time represents at least an order of magnitude improvement over that reported for cointercalated TiS_2 (>600 °C), which ranged from several days to several weeks[23] at 220–240 K. The intercalation rate for NH_3 alone was difficult to determine from the height of a column of TiS_2 (500 °C) in liquid ammonia as the N_2 evolved during the reaction interfered with the measurements. The gas evolution proceeded very gradually even at room temperature, contrasting with the sustained bubbling found in the case of TiS_2 (>600 °C). Insertion of the molecules was verified by X-ray diffraction while pressure measurements during thermal deintercalation gave y' = 0.29 and y'' = 0.52 for a $(NH_4)_{y'}(NH_3)_{y''}TiS_2$ sample obtained from a 3-month ammoniation of TiS_2 (500 °C). This NH_4^+ fraction is larger than that measured for ammoniated TiS_2 (>600 °C) (y' = 0.19–0.22).[21]

Table I. Cell Parameter Values for the Studied Compounds

compound	a, Å	c, Å	$\Delta 2\theta$ (00n)	ΔvdW, Å
TiS_2 (500 °C)	3.4058 (7)	5.693 (1)	0.126	
$(NH_4)_{0.29}(NH_3)_{0.52}TiS_2$	3.4179 (7)	26.482 (6)	0.239	3.134
$Eu_{0.10}(NH_3)_{0.56}TiS_2$ (cointercalate)	3.4232 (6)	26.463 (8)	0.272	3.128
$Eu_{0.10}(NH_4)_{0.20}(NH_3)_{0.20}TiS_2$ (preintercalate)	3.4256 (4) 3.4286 (2)	25.898 (5) 25.500 (6)	0.190 0.279	2.940 2.807
$Eu_{0.10}TiS_2$ from cointercalate (TiS_2-like reflections)	3.4046 (7)	5.713 (3)	0.288	0.020
$Eu_{0.10}TiS_2$ from preintercalate	≈3.41	$d(00n) \approx 6.24$	≈1.34	≈1.10[a]

[a] See text.

Eu–Ammonia Intercalation Compounds. The properties described below did not appear to vary with either the room-temperature annealing period following the intercalation process or the time elapsed after the samples were loaded into appropriate containers; they may then be taken as characteristic of phases in equilibrium.

X-ray Diffraction. Table I summarizes the X-ray diffraction results for the various compounds studied. Ammonia containing samples essentially exhibit a 3R-type structure with $c/3$ equaling the TiS_2 c parmeter plus the ≈3 Å van der Waals gap dilation due to the molecules. The actual value of c depends upon the relative presence of the four possible intercalant species, NH_3, NH_4^+, Eu^{2+}, and Eu^{3+}, which have radii of 1.67, 1.43, 1.10, and 0.95 Å, respectively. The more subtle changes in the a parameters reflect the extent of charge transfer from guest to host.[23]

The c parameter is slightly smaller and a slightly larger in the cointercalated $Eu_{0.10}(NH_3)_{0.56}TiSi_2$ compound than in $(NH_4)_{0.29}(NH_3)_{0.52}TiS_2$. The (003) peak is quite broad in both cases, with that of the ammoniated disulfide being slightly narrower. The implication is that NH_3 and NH_4^+ populate the interlayer gaps more homogeneously than do NH_3 and $Eu^{2+,3+}$. A very small amount of diffuse scattering due to a stage-2-like phase[24] was detected in both com-

(23) (a) Whittingham, M. S.; Thompson, A. H. *J. Chem. Phys.* **1975**, *62*, 1588. (b) Chan, C. T.; Kamitakahara, W. A.; Ho, K. M.; Eklund, P. C. *Phys. Rev. Lett.* **1987**, *58*, 1528.

(24) (a) McKelvy, M. J.; Glaunsinger, W. S. *J. Solid State Chem.* **1987**, *67*, 142. This reference's diffraction data on $(NH_4)_{0.24}TiS_2$ and its 85% reammoniated $(NH_4)_{0.24}(NH_3)_{y'}TiS_2$ compound imply that complex structural variations accompany NH_3 deintercalation and reintercalation. For example, considerating the d = 7.57 Å peak observed in their reintercalated compound as a simple stage-2 reflection implies a vdW gap expansion of 3.75 Å, which is significantly larger than the 2.9–3.2 Å expected from the NH_4^+ and NH_3 diameters, so that a more likely explanation would be the presence of other phases. The same comments could apply to the very weak d = 7.71 Å scattering in the present work's $(NH_4)_{0.29}(NH_3)_{0.52}TiS_2$. (b) Young, V. G.; McKelvy, M. J.; Glaunsinger, W. S.; Von Dreele, R. B. *Solid State Ionics* **1988**, *26*, 47.

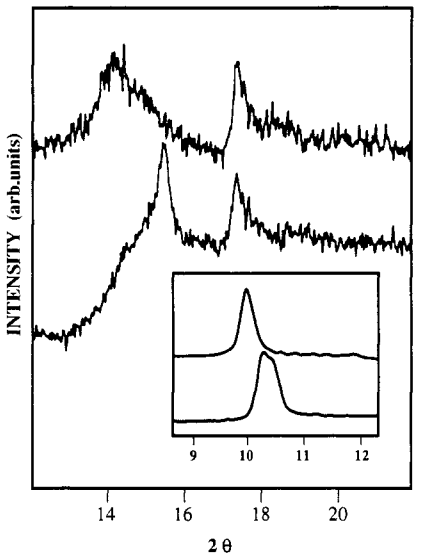

Figure 2. Section of the powder diffraction pattern (λ = 1.54056 Å) showing the first (00*l*) peak in the $Eu_{0.10}TiS_2$ compounds: a broad peak centered at $2\theta \approx 14.18°$ ($d \approx 6.24$ Å) is found in the preintercalate derived material (top) while the TiS_2 (001) appears along with some lower 2θ diffuse scattering in the cointercalate (bottom). The first-order $\sqrt{3}a \times \sqrt{3}a$ superlattice reflection ($2\theta \approx 17.4°$, $d \approx 5.1$ Å) is also shown. Inset: the (003) for $Eu_{0.10}(NH_3)_{0.56}TiS_2$ (top) and $Eu_{0.10}(NH_4)_{0.20}(NH_3)_{0.20}TiS_2$ (bottom), the latter of which consists of two peaks.

pounds at d = 7.48 and 7.71 Å, respectively. The appearance of this minority phase is attributable[21,24] to the diffusion of NH_3 molecules facilitated by the inert gas under which these samples are stored.

Two families (phases A and B) of stage-1 reflections are consistently found in the preintercalated Eu compounds (see Figure 2 inset). This feature may be related to the presence of NH_4^+, normally nonexistent in cointercalated compounds of the same Eu concentration. Table II displays a typical powder diffraction pattern from $Eu_{0.10}(NH_4)_{0.20}(NH_3)_{0.20}TiS_2$. The lattice parameters were refined assuming the pattern to be a sum of two sets of peaks. As the two sets overlap and the peaks may be slightly shifted in position and broadened as an effect of the mixing of the two types of unit cells,[25] a satisfactory fit including all the reflections cannot be expected. Refining the data with the two sets considered as either disjoint or overlapping, however, yields consistent results, and the smaller c parameter family (A) is always found to have a slightly larger a. This set A also has a much wider (003) peak. The intercalants in phase A, as compared to those in B, can therefore be characterized as being more ionic, transferring more charge, and having less uniform interlayer gap concentrations. The cell-parameter and peak-width trends observed in the ammoniated and cointercalated compounds imply that A may be associated with microdomains of mainly NH_3 and europium and B with mainly NH_3 and NH_4^+. This is physically intuitive as the europium ions can be expected to repel the protons.

$Eu_{0.10}TiS_2$ obtained upon deintercalation of ammonia exhibits a considerable amount of disorder with the c-axis structure apparently depending on the nature of the ammoniated precursors. Common to all samples, on the other hand, is a small peak at $2\theta \approx 17.4°$ ($d \approx 5.1$ Å), which indexes as the primary reflection of a $\sqrt{3}a \times \sqrt{3}a$ superlattice. Such a structure, already observed in other related intercalated systems,[26] is conceivable at the given low Eu concentration considering that $\sqrt{3}a$ is significantly larger than the nearest neighbor distance in Eu metal.[27] Figure 2 shows the relevant section of the diffraction data.

Table II. Powder Diffraction Data for $Eu_{0.10}(NH_4)_{0.20}(NH_3)_{0.20}TiS_2$[a]

hkl	d_{obs} Å	d_{calc}, Å A	d_{calc}, Å B	intensity
003	8.50	8.50		100
	8.65		8.63	51
006	4.25	4.25		2
	4.31		4.32	4
102	2.892	2.892	2.892	25
104	2.691	2.692	2.697	2
105	2.573		2.574	74
	(2.559)	(2.566)		17
107	(2.291)	(2.302)		1
	2.310		2.314	3
108	2.186		2.187	19
	(2.163)	(2.173)		15
1010	1.952		1.951	5
	(1.924)	(1.935)		2
110	1.714	1.714	1.713	26
113	1.6806	1.6807	1.6799	19
1013	(1.6570)	(1.6368)	(1.6537)	4
202	1.4734	(1.4748)	1.4736	3
205	1.4249	1.4256	1.4259	11
208	1.3488		1.3484	3
	(1.3441)	(1.3459)		1
2010	1.2872	(1.2831)	1.2870	<1
212	1.1174	(1.1181)	1.1170	3
215	1.0960	1.0962	1.0958	6
218	(1.0598)	(1.0587)	(1.0594)	4
300	0.9895	0.9899	(0.9888)	3
303	0.9831	0.9832	(0.9824)	1
304	0.9783	0.9781	(0.9775)	<1

[a] The cell constants from the best "two-set" refinement are: for A, a = 3.4290 (6) Å, c = 25.50 (1) Å; for B, a = 3.4253 (6) Å, c = 25.896 (7) Å. The observed d values in parentheses were not included in this particular refinement and were indexed according to the results of an all-inclusive but less satisfactory fit (which consistently gave a = 3.428 (1) Å, c = 25.44 (3) Å for A, and a = 3.4258 (6) Å, c = 25.93 (2) Å for B). The calculated d's in parentheses are given as a comparative reference where deemed helpful. Indexes followed by a brace correspond to two lines of d values.

Preintercalate-derived compounds give a very broad, asymmetric peak at $2\theta \approx 14.18°$ ($d \approx 6.24$ Å). The rest of the pattern is accordingly difficult to index. Line-shape modeling of the $d \approx 6.24$ Å peak reveals the presence of lower d contributions so that this peak can be interpreted as representing a distribution of stages. The 6R-type, stage-2 structure of low-concentration alkali metal–TiS_2 intercalates[10,28] suggests that $Eu_{0.10}TiS_2$ is at least stage 2 with a corresponding vdW gap width of ≈6.79 Å (from stage-2 $d(002)$ = 6.24 Å). This vdW width approaches that found in $Na_{0.15}TiS_2$ (=6.93 Å) as can be expected from the similarity between the ionic radii of sodium and europium cations.[10,29] The c-axis repeat distances for the higher stages are easily calculated to yield stage-n $d(00n)$ values clustered below d = 6.24 Å (e.g., stage-3 $d(003)$ = 6.06 Å, stage-4 $d(004)$ = 5.97 Å).

Some lower 2θ diffuse scattering is also found in the cointercalate-derived compound, but the diffraction pattern is dominated by TiS_2-like reflections. Refinement of the lattice parameters corresponding to these peaks yields

(25) Hendricks, S.; Teller, E. *J. Chem. Phys.* **1942**, *10*, 147. See also ref. 30.

(26) (a) Suter, R. M.; Shafer, M. W.; Horn, P. M.; Dimon, P. *Phys. Rev. B.* **1982**, *26*, 1495. (b) Makrini, M. E.; Guerard, D.; Lagrange, P.; Hérold, A. *Physica B* **1980**, *99*, 481.

(27) (a) Wells, A. F. *Structural Inorganic Chemistry*; Clarendon Press: London 1984; p 1283. (b) Klemm, W.; Bommer, H. *Z. Anorg Chem.* **1937**, *231*, 153.

(28) Rouxel, J. In *Intercalated Layered Materials*; Levy, F., Ed.; Reidel: Dordrecht, 1979; p 201.

(29) Top, L. H. Thesis, Nantes, France, 1981.

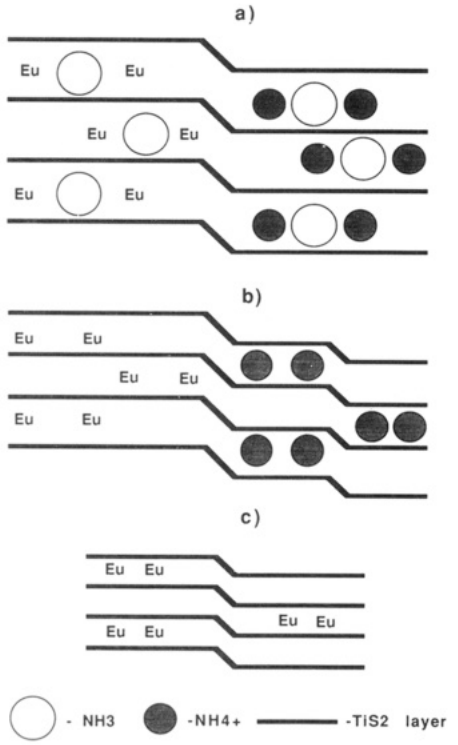

Figure 3. Schematic representation of possible Daumas–Hérold domain formation and staging in the preintercalate series of compounds: (a) $Eu_{0.10}(NH_4)_{0.20}(NH_3)_{0.20}TiS_2$ (phase A, left; B, right); (b) the assumed intermediate $Eu_{0.10}(NH_4)_{0.20}TiS_2$ after NH_3 deintercalation; (c) $Eu_{0.10}TiS_2$.

an a essentially equal to and a c slightly larger than those of the plain disulfide (Table I). The (001) (at $2\theta = 15.498°$) is markedly broadened. It therefore seems that this material consists of separate intercalated and unintercalated regions with elastic strains in the former causing deformations in the latter. This is very similar to the case of stage $n > 7$ potassium graphite[30] compounds, which are characterized by high c-axis disorder and the reappearance of the graphite (002).

The above results can be interpreted within the Daumas–Hérold (DH) domain model of staging[31] where every interlayer gap is globally filled but locally forms staged structures following the arrangement of intercalant islands. Staging transitions in this model are explained via the lateral displacements of the intercalants. Figure 3a is a schematic representation of how DH domains might occur in the preintercalate $Eu_{0.10}(NH_4)_{0.20}(NH_3)_{0.20}TiS_2$. Layers of europium cations and NH_3 and of NH_3 and NH_4^+ are shown to form laterally separate domains (phases A and B). It is known that the ionic compound $(NH_4^+)_yTiS_2^{y-}$ has a predominantly stage-2-like structure,[24] and it is conceivable that the same rearrangement of the NH_4^+ occurs in $Eu_{0.10}(NH_4)_{0.20}TiS_2$ upon the departure of 0.20 mol of NH_3 (Figure 3b). Formation of stage $n \geq 2$ structures in $Eu_{0.10}TiS_2$ (stage-2 shown in Figure 3c) may be due to an in-plane condensation of the europium intercalants induced by the volume reduction (the collapse of the vdW gap) that follows the deintercalation of the remaining ammonium; contraction of the vdW gap then also permits registry of the europium intercalants with the hexagonal host lattice. In the cointercalated compound $Eu_{0.10}(NH_3)_{0.56}TiS_2$, the absence of NH_4^+ removes the constraint on the lateral distribution of the europium, implying both low in-plane concentrations and weak out-of-plane correlations, the latter of which may explain the reappearance of the TiS_2 (001) in the derived $Eu_{0.10}TiS_2$. Observation of a $\sqrt{3}a \times \sqrt{3}a$ reflection and the TiS_2 lines suggests that the cations tend to coalesce when NH_3 is removed, leaving behind empty TiS_2 gaps.

(30) Huster, M. E.; Heiney, P. A.; Cajipe, V. B.; Fischer, J. E. *Phys. Rev. B* **1987**, *35*, 3311.
(31) (a) Daumas, N.; Hérold, A. *C. R. Acad. Sci.* **1969**, *268*, 373. (b) Kirczenow, G. *Phys. Rev. Lett.* **1985**, *31*, 5376.

Table III. Curie–Weiss Law Fit Parameters

$\chi = C/(T - \theta)^a$

compound	cycle	C, emu mol^{-1} K	θ, K
$Eu_{0.10}(NH_4)_{0.20}(NH_3)_{0.20}TiS_2$	w[b]	7.3	−6
(preintercalate)	c	7.2	−6
$Eu_{0.10}TiS_2$ from preintercalate	w	7.9	−7
	c	7.8	−5
$Eu_{0.10}(NH_3)_{0.56}TiS_2$ (cointercalate)	w	7.0	1
$Eu_{0.10}TiS_2$ from cointercalate	w	7.2	0
	c	7.3	−4

[a] It should be noted that the Curie–Weiss (CW) law was used to fit the data only to obtain general, semiquantitative information on the studied compounds. This works because the Eu^{2+} susceptibility dominates the non-CW Eu^{3+} and d^1 contributions; the Weiss constant θ thus obtained is not necessarily related to the intensity and sign of the magnetic interactions. [b] w = warming, c = cooling cycle.

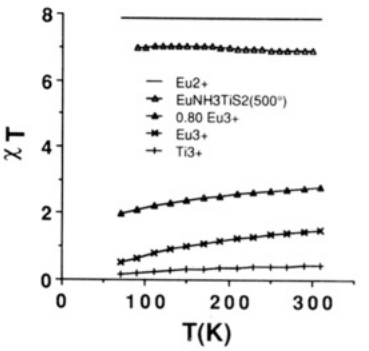

Figure 4. χT per mole of Eu vs temperature for $Eu_{0.10}(NH_4)_{0.20}(NH_3)_{0.20}TiS_2$ (preintercalated compound) as compared to χT for the 80% trivalent case calculated from the $0.2\chi(Eu^{2+}) + 0.8\chi(Eu^{3+})$ function used to model the susceptibility data for a similar Eu concentration TiS_2 (> 600 °C) compound in ref 22. The χT curves from the independent Eu^{2+} ($S = {}^7/_2$), Eu^{3+} (after ref 32) and Ti^{3+} (after ref 33) functions are also given as references.

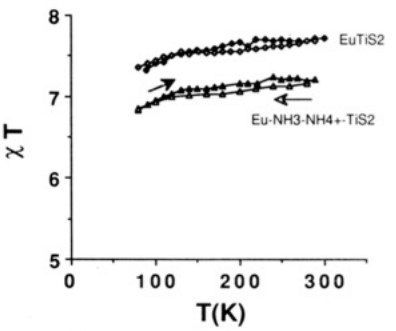

Figure 5. T dependence of χT for the ammonia-containing and the ammonia-free Eu intercalates prepared from preammoniated TiS_2.

Magnetic Susceptibility. The magnetic susceptibility data from the various samples are summarized in Figures 4–6 and Table III. The following observations can be made:

χT as measured in the present work is larger than reported for the Eu intercalation compounds of TiS_2 (>600 °C). Attributing the overall susceptibility to Eu^{2+} and Eu^{3+}

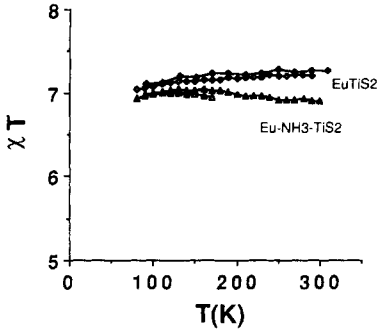

Figure 6. T dependence of χT for the ammonia-containing and the ammonia-free Eu intercalates obtained by cointercalation. The solid symbols represent data from the warming cycle, the nonsolid from cooling.

contributions (see Figure 4), the implication is that Eu intercalated into TiS_2 (500 °C) is predominantly divalent rather than trivalent as found in previous studies.[22]

The details of the T dependence of χT cannot be accounted for by a simple weighted sum of the Eu^{2+} and Eu^{3+} functions,[32] which was the model used in previous work to evaluate the cations' relative abundances.[22] The curves for $Eu_{0.10}(NH_3)_{0.20}(NH_4)_{0.20}TiS_2$ and both varieties of $Eu_{0.10}TiS_2$ exhibit an increase in slope below $T \approx 150$ K (Figures 5 and 6). The slopes of the higher T segment of the curves are in fact larger than can be expected from the small Eu^{3+} fraction (lower bound) given by the room-temperature susceptibility. A complete model would then have to include contributions that suppress χT, e.g., antiferromagnetic interactions and the localization of Eu-donated electrons on the Ti atoms considered as octahedrally coordinated paramagnetic d^1 centers.[33] The latter possibility is suggested by the EPR behavior (see below). Applying the localization correction to the superposed Eu^{2+} and Eu^{3+} susceptibilities, however, overestimates the Eu^{3+} fraction (upper bound). The limits on the corresponding Eu^{2+} content are then (0.74, 0.90) in the preintercalate $Eu_{0.10}(NH_3)_{0.20}(NH_4)_{0.20}TiS_2$, increasing to (0.83, 0.98) in its derived $Eu_{0.10}TiS_2$, and (0.74, 0.90) for the cointercalate-derived $Eu_{0.10}TiS_2$. The Eu is thus at least 74% divalent in the present compounds as opposed to 60–80% *tri*valent as found previously.[22] The $Eu_{0.10}(NH_3)_{0.56}TiS_2$ case is slightly different in that the high-T slope of χT is negative (Figure 6); this may be due to the Eu^{2+} spins coupling differently following their more random arrangement in this compound. The Eu^{2+} content is estimated to be $\approx$0.85.

The possibility of $Eu(NH_2)_2$ contamination (Eu is divalent in the amide) of the present samples has been considered. Calculating from the raw data and sample mass and assuming the intercalation product to be essentially trivalent, we find that 70% of the signal should be attributable to $Eu(NH_2)_2$, i.e., 30–40% of the original Eu mass should have gone into amide formation. This is completely inconsistent with the absence of both visible and X-ray evidence for the amide as well as with the observed rapid intercalation rate, the vdW gap expansion, and the EPR data (see below).

Deintercalation of NH_3/NH_4^+ results in an increase of the susceptibility, i.e., the Eu^{2+} content, in agreement with ref 22 and consistent with the absence of Eu amide as the heating of $Eu(NH_2)_2$ yields the nitride[34] where Eu is trivalent. A semiquantitative index to this increase is given by the Curie–Weiss law fit parameters for the χ^{-1} data (Table III), which show this effect to be larger in the preintercalate case.

Figure 7. EPR spectra of (from top to bottom): $Eu_{0.10}(NH_4)_{0.20}(NH_3)_{0.20}TiS_2$ (preintercalate) at 100 and 300 K; $Eu_{0.10}(NH_3)_{0.56}TiS_2$ (cointercalate) at 300 K; and $Eu_{0.10}TiS_2$ (preintercalate) at 100 and 300 K.

A reproducible hysteresis in χT is observed with thermal cycling for $Eu_{0.10}(NH_3)_{0.20}(NH_4)_{0.20}TiS_2$ and the $Eu_{0.10}TiS_2$ compounds. The effect is weak and barely noticeable in the original χ data but lies well outside the error bars for χT. The moment is found to be higher when warming than when cooling.

The above observations demonstrate the complexity of the magnetic behavior of these materials. The increased susceptibility found after ammonia removal illustrates a sensitivity to the redox processes occurring in the vdW gap, while the weak hysteresis is suggestive of kinetics.

EPR Measurements. EPR signals were observed for all the samples considered in the present study. On the contrary, no signal was detectable in any of the TiS_2 (>600 °C) intercalation compounds,[22] presumably because of extreme line broadening due to rapid electronic exchange between Eu^{2+} and Eu^{3+} via the TiS_2 conduction band.

Figure 7 shows a representative set of lines. The broad, asymmetric room-temperature signal for the preintercalate $Eu_{0.10}(NH_4)_{0.20}(NH_3)_{0.20}TiS_2$ is resolved as a superposition of eight lines at 100 K; the integrated absorption curves at different temperatures are consistent with the susceptibility data. Deintercalation of NH_3 and NH_4^+ leads to a further broadening of the ambient temperature signal, which shows a change of shape but no appreciable sharpening at low T. The cointercalate $Eu_{0.10}(NH_3)_{0.56}TiS_2$ gives a room-temperature signal resembling that of the preintercalate but consisting of different relative contributions from the several lines present; this slight difference may well be related to the dissimilar behavior of the respective susceptibilities. It is also probable that the character of the signals measured is related to the degree of structural order and the symmetry of sites in the samples. A quan-

(32) Saez Puche, R.; Norton, M.; White, T. D.; Glaunsinger, W. S. *J. Solid State Chem.* **1983**, *50*, 281.
(33) Mabbs, F. E.; Machin, D. J. *Magnetism and Transition Metal Complexes*; Chapman and Hall: London, 1973; p 68.
(34) Hadenfeldt, V. C.; Jacobs, H.; Juza, R. *Z. Anorg Chem.* **1970**, *379*, 144.

titative analysis of the data is being carried out and will be discussed in a later paper. We point out that the temperature-independent 1-kG wide, $g = 2.015$ signal[35] characteristic of $Eu(NH_2)_2$ was not observed.

Conclusion

We have shown that preintercalated and cointercalated Eu–ammonia–TiS_2 have dissimilar structures and magnetic behavior and yield different Eu–TiS_2 phases. Furthermore, the measured properties were found to be more complex than shown in previous studies.[22] The main finding of the present work, however, is that the Eu intercalation rate and the nature of the yielded compounds depend quite strongly on the way TiS_2 is prepared.

Ammoniated TiS_2 (500 °C) contains more ammonium than TiS_2 (>600 °C), but the average Eu oxidation state in the europium intercalated TiS_2 (500 °C) is found to be lower. Since the presence of NH_4^+ results from the oxidation of intercalated ammonia,[36] we infer that oxidation in the vdW gap is a complex process that possibly involves mechanisms that differ according to whether the guest is a molecule or an ion. The cases of NbS_2 and TaS_2 support this assertion. NbS_2 in its limiting, stoichiometric 2H form is found to contain $0.25NH_4^+$ after pure ammonia intercalation[37a] but intercalates only negligible amounts of Eu–NH_3 after several months.[37b] On the other hand, while the Nb-rich 3R polytype does intercalate europium with the 0.17Eu compound containing significant amounts of Eu^{3+}, its intercalation with pure ammonia appears to be quite difficult.[37c] In the same vein, 2H-TaS_2 easily intercalates ammonia[38a] and contains $\approx 0.15NH_4^+$, whereas 1T-TaS_2, which has been shown to contain interstitial Ta,[38b] intercalates europium predominantly in its trivalent state but is less than 10% intercalated and contains no ammonium after several days immersion in liquid ammonia.[38c] These examples point out the intimate relationship between oxidation and intercalation and suggest a strong dependence of these on both cation stoichiometry defects and coordination.

TiS_2 (500 °C) from the elements in stoichiometric proportion readily intercalates 0.10Eu in <1 h at 228 K. On the other hand, completion of Eu intercalation in TiS_2 (>600 °C) prepared following the procedure recommended by previous workers[20,22] takes up to several weeks at the same temperature. Our own experience with nearly stoichiometric TiS_2 (>600 °C) shows that the decomposition of Eu–NH_3 solutions into Eu amide is favored in this case because of the long intercalation time. As the particle sizes of the two types of disulfide used in these intercalation studies are basically similar, the dramatically increased rate observed in TiS_2 (500 °C) should be due to more than just a smaller aspect ratio. Further, since our TiS_2 (>600 °C) was prepared from the same Ti powder (as opposed to the Ti wire of others[20,22]), the difference in intercalation rates cannot be ascribed to unequal impurity levels.

Our results indicate rather that TiS_2 (500 °C) has less defects (interstitial Ti) than TiS_2 (>600 °C). The former has no luster while the latter resembles a metal. TiS_2 (500 °C) has a lower magnetic susceptibility that exhibits a weak T dependence below ≈150 K (note that the magnetic susceptibility of *perfectly* stoichiometric TiS_2 is actually unknown). Its cell volume is also smaller, implying that it has less excess Ti, a subtle difference that would be difficult to detect by chemical analysis. Moreover, the metal-type reflectance exhibited by TiS_2 (>600 °C) in the EPR microwave cavity is significantly less in the TiS_2 (500 °C) case. Interestingly, the Eu-containing phases prepared by using TiS_2 (500 °C) have no pronounced metallic character either, although the amount of charge transfer is large (0.21–0.33 electron/TiS_2 formula). This suggests the occurrence of charge localization, consistent with the susceptibility data that indicate that electrons localized on the Ti have to be considered.

The presence of more defects in TiS_2 (>600 °C) may be explained as follows. First, at the >600 °C temperatures necessitated by the use of "purer" but more slowly reacting Ti wire, titanium atoms have a higher probability of being excited into the vdW gap. Remaining below ≈600 °C has then been recommended.[12a] Second, TiS_2 tends to lose sulfur at these elevated temperatures[12b] so that an excess of it has to be provided.[20] However, an excess of sulfur can lead to the formation of TiS_3, a side product assumed to transform into TiS_2 during the second step of the TiS_2 (>600 °C) preparation. It has recently been shown[38] that NbS_2 obtained from NbS_3 contains a large amount of defects (excess Nb), and it is quite possible that the TiS_2 resulting from the thermolysis of TiS_3 is defected in the same way. This intermediate process and the use of elevated temperatures distinguish the TiS_2 (>600 °C) from the TiS_2 (500 °C) preparation method and may very well account for the differences described in this paper.

In conclusion, we would like to point out that ammonia and Eu intercalation can be viewed as a method for the detection of defects such as interstitial Ti in TiS_2. We have shown accordingly that TiS_2 (500 °C) is possibly more stoichiometric than TiS_2 (>600 °C). Its less metallic character is consistent with the semiconducting behavior expected of the ideal disulfide. Its faster reaction with Eu implies an optimization of its properties as an intercalation host and a battery cathode material.

Acknowledgment. We thank M. Danot and W. Glaunsinger for many helpful discussions and J. Rouxel for valuable suggestions. The Eu metal used in the first few preparations was generously provided by W. Glaunsinger.

Registry No. Ti, 7440-32-6; Eu, 7440-53-1; NH_3, 7664-41-7; TiS_2, 12039-13-3; $Eu_{0.10}TiS_2$, 125648-81-9; sulfur, 7704-34-9.

(35) Kokoszka, G. F.; Mammano, N. J. *J. Solid State Chem.* **1970**, *1*, 227.

(36) Colombet, P.; Cajipe, V. *Eur. J. Solid State Inorg. Chem.* **1989**, *26*, 255.

(37) (a) Dunn, J. M.; Glaunsinger, W. S. *Solid State Ionics* **1988**, *27*, 285. (b) Subba Rao, G. V.; Shafer, M. W.; Tao, L. J. *Mater. Res. Bull.* **1973**, *8*, 1231. (c) Cajipe, V. Unpublished results.

(38) (a) Schollhorn, R.; Zagefka, H. D. *Angew. Chem., Int. Ed. Engl.* **1977**, *16*, 199. Also, private communication, Diebolt, L.; Glaunsinger, W. S. (b) DiSalvo, F. J.; Waszczak, J. V. *Phys. Rev. B* **1980**, *22*, 4241. (c) Unpublished results, Cajipe, V.; Molinié, P.; Gourlaouen, V.; Colombet, P.

(39) Kurdi, M.; Marie, A. M.; Danot, M. *Solid State Commun.* **1987**, *64*, 395.